

High Efficiency Solar Cells Base on Organic-inorganic Perovskites Materials

Zainab. R. Abdulsada
Dept. of Physics /College of Science /
University of Thi Qar
Nasiriyah, Iraq
Email: Zainab_rah.ph@utq.edu.iq

Samir M . AbdulMohsin
Dept. of Physics /College of Science /
University of Thi Qar
Nasiriyah, Iraq
Email: samer.mahdi75@gmail.com

Abstract— In this research (PCBM) was used as Electron Transport Material (ETM) and (P3HT) as Hole Transport Material (HTM), where used with the perovskite ($\text{CH}_3\text{NH}_3\text{PbI}_3$) and changed the thickness ETM from (100nm) to (2600). And changed the effective density of states (CB, VB) (from $2.20\text{E}12$, to $=2.20\text{E}20$ for $\text{CH}_3\text{NH}_3\text{PbI}_3$) with this variable an efficiency of 9.74% was obtained at 263.15(k). By using SCAPS simulation software.

Keywords— Perovskite, efficiency, Electron Transport Material (PCBM), Hole Transport Material (P3HT).

I. INTRODUCTION

In recent years, organic-inorganic perovskite solar cells have attracted great interest in the photovoltaic research community due to their ease of manufacturing, low production costs, superb light harvesting characteristics and high performance, making them more preferable than other current solar cell materials. Solar cells have achieved extremely high-power conversion efficiencies (PCEs) of more than 20 percent in solution-processed perovskite (PSC), but practical application of this photovoltaic technology requires further advances in both long-term stability and large-area demonstration materials. The perovskite-based type of solar cells have gained ever-increasing prominence in the type solar cells, because of their outstanding physical properties:

(1) strong optical absorption (2) high charge carrier mobility (3) high photovoltaic conversion efficiency. Methylammonium (MA) lead halide (e.g. $\text{CH}_3\text{NH}_3\text{PbI}_3$), the most commonly employed material in (PSCs) solar cells, was reported to have high absorption coefficients (direct bandgap ~ 1.55 eV) as well as high mobilities for electrons and holes. [1] SCAPS analyzes the physics of the model and defines the recombination profiles, the electric field distribution, the transport mechanism of the carrier, and the individual current densities. The impact of various layer characteristics on cell performance, such as thickness and defect density, have been thoroughly investigated. The thickness of the absorber and buffer (TiO_2) layers influences the short-circuit current density (J_{sc}) and

efficiency (PCE) of solar cells. The PSCs use organic and inorganic materials of different forms, such as TiO_2 , ZnO , SnO_2 , and PCBM, such as ETM [2][3]. By filling pinholes and vacancies between perovskite grains, PCBM plays a critical role in improving the efficiency of the light-absorbing layer, resulting in a film with wide grains and fewer grain borders [4].

II. PEROVSKITE SOLAR CELLS

Nature published an article on a perovskite solar cell with an efficiency greater than 10% in 2012. Since then, due to their high performance, low manufacturing costs, and strong marketing ability, Perovskite solar cells have attracted a lot of attention [5]. The composition of perovskite solar cells consists generally of 5 layers which are a cathode layer of silicon, the anode-based layer of the hole material (HTM), perovskite layer and, anode layer (FTO/ITO). A typical perovskite solar cell with a planar structure is shown in Figure.1. The perovskite layer is used in the unit, where photon excitation occurs, as a light absorber. The produced electrons and holes are separated and transferred to the ETM layer and HTM layer respectively. The function of the ETM layer is that electrons and block holes are extracted and transferred. The HTM layer is used to remove and pass holes and block electrons. This implies high electron mobility in the ETM layer, high mobility in the HTM layer for holes, and appropriate band offsets between the ETM layer/perovskite layer/HTM layer necessary for high efficiency. [6][7]. The major processes of charge transport in perovskite solar cells are shown in Figure.2. The green arrows are desirable energy transfer processes, including photon excitation, the transport of electrons from the perovskite layer to the ETM layer, and the transport of holes from the perovskite layer to the HTM layer. The red arrows show the unwanted power loss processes for perovskite solar cells involving the combination of charging carriers, ETM layer back electron

flow, and HTM layer hole flow with the perovskite layer [8].

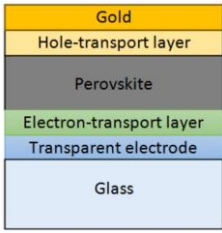


Figure.1. The configuration of perovskite solar cell with planar structure [9].

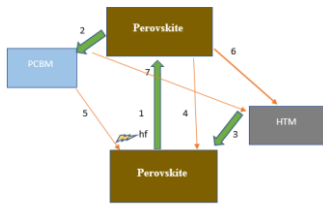


Figure.2. Schematics showing of charge transport in perovskite solar cells [9]

III. CHARGE CARRIERS IN PEROVSKITE MATERIAL (CH₃NH₃PbX₃)

A challenge has been the determination of charge carriers in organic-inorganic hybrid perovskite solar cells. The existence of both organic and inorganic components is largely due to this Edri et al[10] experimentally examined this ambiguity about the existence of carriers in perovskite material . It was found that the lead halide perovskite solar cells (thin film and/or inert mesoporous configuration) operate generally as p-i-n junction. An intrinsic semiconductor material has a p-i-n junction sandwiched between an extrinsic semiconductor type p and n. Their study was carried out on a solar cell with mixed halide lead based perovskite, CH₃NH₃PbI₃-xClx absorber., Minemoto etal. and Tanaka et al [11]. They found that a typical Wannier-type exciton is the dominant charge carrier in lead halide perovskite. This is similar to the type of charge carriers observed in inorganic materials. Wannier type excitons occur when the electric field screening tends to reduce the Coulomb interaction between electrons and holes. The screening reduces the binding energy of the electron-hole pair and makes them move independently, unlike Frenkel excitons which occur in organic materials [12].

IV. NUMERICAL EMULATION

Simulation is a crucial technique for realizing a deep insight into the physical activity, the viability of the suggested physical interpretation, and the effect of physical changes on the solar cell devices' performance. Different models of simulation exist for solar cell simulation (SCAPS, AMPS, SCAP, etc). SCAPS is a one-dimensional program for simulation with seven input layers of semiconductors manufactured by a group of researchers from Ghent University, Belgium (Solar cell power simulator) [13]. It is not possible to build a solar cell without stimulatory operation, as time and resources are wasted. It does not only minimize the risk, time, and money but also analyzes the properties of the layers and their function to maximize the efficiency of the solar cell. To simulate a computer all the basic input parameters should be well specified to function as a real counterpart. The different structure has been used by perovskite-based solar cells with inorganic semiconductor solar cells, such as CIGS, and exciting form Wannier is contained in perovskite. Thus, SCAPS like a 1D

simulator can be used to model solar cells based on perovskite

[14].

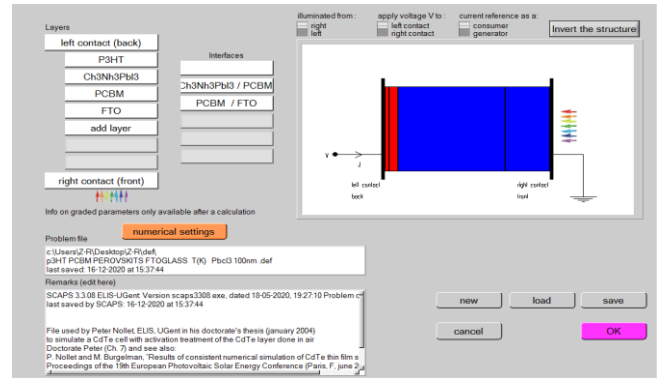


Figure 3. SCAPS panel showing the FTO/PCBM /CH₃NH₃PbI₃/P3HT heterojunction solar cells definition

SCAPS is a numerical solution of the two poisson equations and the continuity equations on the limits of one dimension or two [15]. Express the following equations.

$$\nabla^2 V = -q / \epsilon (p - n + N_D - N_A) \dots \dots \dots (1)$$

$$\nabla \cdot J_p = q(G - R) \dots \dots \dots (2)$$

$$\nabla \cdot J_n = q(R - G) \dots \dots \dots (3)$$

$$J_p = -q \mu_p P \nabla U_p - KT \mu_p \nabla p \dots \dots \dots (4)$$

$$J_n = -q \mu_n n \nabla V_n + KT \mu_n \nabla n \dots \dots \dots (5)$$

$$V_p = V - (1 - \gamma) \Delta G / g \dots \dots \dots (6)$$

$$V_n = V + \gamma \Delta G / g \dots \dots \dots (7)$$

Equations (1) Calculates the amount of change in voltage as a result of the difference in the density of the charge in three directions. The higher it is, the more volatile, but stable with time, and this causes an increase in the movement of the charge and the speed of its transfer in the center or the area of depletion.

Equation 2 is the net gain of the current as a result of the processes of generation and recombination, the final net represents the current and when taking a grad is to reveal the extent of change or activity of this process in the three dimensions

Equations 5 and 6 represent the current density of the hole and the electron. Where Vb and Vn are the potential effectives expressed in Equations 6 and 7. ΔG is band structure variation, μn, μp represents electron and hole mobility, respectively.

V. SOLAR CELL DEVICE CHARACTERIZATION PARAMETERS

The main parameters that are used to characterize the performance of solar cells are the (Power Conversion Efficiency, (η) ,the short-circuit current density, (Jsc) .

A. Short-Circuit Current Density (Jsc)

The short-circuit current density (is the maximum photogenerated current delivered by a solar cell when the terminals of the solar cell are in contact with each other (i.e.

short-circuited)). The solution for (J_{sc}) can be gotten from the net current density($J(V)$) in the solar cell given as.

$$J(V) = J_{sc} - J_{dark}(V) \quad (8)$$

where

$$J_{dark}(V) \text{ is the dark current density. This is given by:}$$

$$J_{dark}(V) = J_0(e^{qv/mk_B T} - 1) \quad (9)$$

Set a solar cell under a standard light source, when the output is in short circuit state, which means the voltage value is 0, the current is the maximum output current called short-circuit current. It is given as:

Or equivalently, the short circuit current given by:

$$J_{sc} = J(V) + J_0(e^{qv/mk_B T} - 1) \quad (10)$$

Where V is the voltage across the junction, T is the absolute temperature, J_0 is the dark saturation current density and m is the ideality factor with values between 1 and 2.

B. Power Conversion Efficiency (η)

Power conversion efficiency (η) is the percentage of incident power transformed into useable electricity by solar cells.

The ratio between the generated maximum power and the incident power is used to calculate the power conversion efficiency.

This is given by:

$$\eta = \frac{P_{max}}{P_{in}} = \frac{J_{sc} V_{oc} FF}{P_{in}} \quad (11)$$

VI. SCAPS SIMULATION OF FTO/PCBM/PEROVSKITE/P3HT

Notice that all simulation parameters are carefully chosen from the recorded experimental data and other literature for each layer of the architecture. Table .1. Summarizes all primary simulation parameters.

Table 1. Material properties of ETM, absorber, and HTM

parameters	FTO	P3HT	CH3NH3PbI3	PCBM
Band gap(ev)	3.500	2.000	1.550	2.000
Electron affinity (ev)	4.000	3.200	3.750	3.900
Dielectric permittivity	9.000	3.000	6.500	3.900
CB effective density of states (1/cm ²)	2.200E+18	1.000E+20	2.200E+13	2.540E+21
VB effective density of states (1/cm ²)	1.800E+19	1.000E+20	2.200E+12	2.540E+21
Electron mobility (cm ² /v.s)	2.000E+1	1.000E-4	2.000E+0	3.400E+2
Hole mobility (cm ² /v.s)	1.000E+1	1.000E+0	2.000E+0	1.000E+1

Table 2: Configure Usage parameters for numerical analysis.

Right contact electrical properties (Au)	
Thermionic emission /surface recombination	10 ⁵
Velocity of electron (cm/s)	
Thermionic emission /surface recombination	10 ⁷
Velocity of hole (cm/s)	
Metal (Au) work function (ev)	5.1
Left contact electrical properties	
Thermionic emission /surface recombination	10 ⁷
Velocity of electron (cm/s)	
Thermionic emission /surface recombination	10 ⁵
Velocity of hole (cm/s)	
the work function of ITO (ev)	4.4

Tables shows the values of the most useful cell parameters required for the simulation. These values have been selected on the basis of or in certain cases realistic projections of theoretical factors, experimental evidence and current literature. Most of the parameters used for the absorber and the thicknesses of the other layers were extracted from the literature while the parameters for other layers in the Table were gotten from the works reported by [16] and [17].

VII. RESULT AND DISCUSSION

The results derived from numerical simulations are discussed in this part. The cell output variations that occur in the cell parameter variance are discussed. The parameters investigated are Effect of the (thickness of ETL Layer, effective density of states, annealing Temperatures, Different Back Contacts) for FTO/P3HT/CH3NH3PbI3/PCBM solar cells device.

A. Effect of the thickness of PCBM on the solar cell.

The absorber layer should be set for optimum thickness to absorb the maximum number of photons and to produce electron-hole pairs. Absorber layer thickness has been ranged from 100nm to 2600nm. When the thickness of the absorber layer increases the longer wavelength of the illumination creates a fair amount of electron-hole pair generation. Figure.4. shows a difference in the thickness of the PV parameter absorber layer. By looking at the JSC / thickness graph we can say that by increasing its thickness JSC , increased and the efficiency is obtained, The Convert the light to excitons depends on the energy gap, and since the thickness increases, this means that the number of excitons generated increases so the current increases to a certain thickness and then decreases due to the decrease in the transmitted radiation due to the darkening with increasing thickness. And that all the light spectrum may be scattered and lost, except for the red color. It reaches deeper depths by penetration, and by converting it into an exciton, the energy gap must be within the spectrum IR. In addition to increase amount of light which absorb inside the absorber layer due to increase the thickness in specific range. The highest value of efficiency is obtained at the thickness of 1200nm.

Table (3) shows the drawing data for variation thickness of PCBM.

Thickness(nm) PCBM	Jsc (mA/cm ²)	Efficiency %
100	8.048111	6.39
200	10.269948	8.18
300	11.115721	8.86
400	11.500374	9.16
500	11.701013	9.32
600	11.816483	9.41
700	11.887713	9.46
800	11.933813	9.49
900	11.964716	9.51
1000	11.985967	9.52
1100	12.000862	9.53
1200	12.011455	9.54
1300	12.019068	9.54
1400	12.024577	9.54
1500	12.028575	9.54
1600	12.031466	9.53
1700	12.033532	9.53
1800	12.034971	9.53
1900	12.035924	9.53
2000	12.036489	9.52
2100	12.036737	9.52
2200	12.036719	9.51
2300	12.036474	9.51
2400	12.036029	9.50
2500	12.035404	9.50
2600	12.034613	9.50

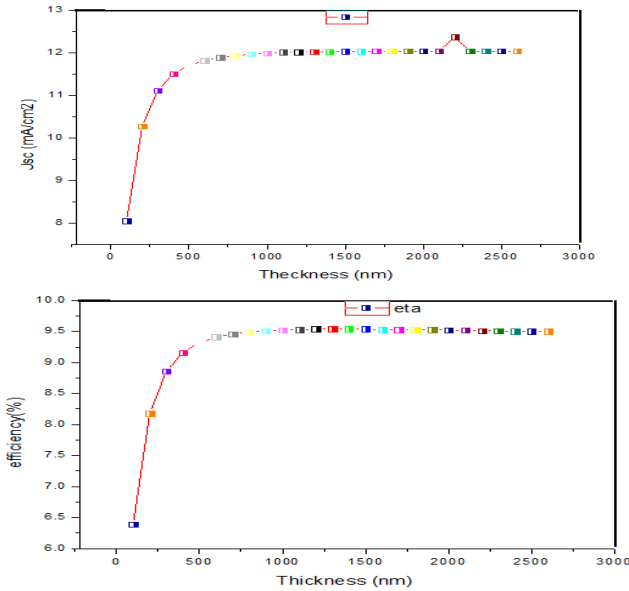


Figure 4. Variation of parameters by varying the thickness of PCBM

B. Effect of the effective density of states on the solar cell

Recently, the low effective mass and consequently the low density of electronic states in the valence band and conduction band found experimentally and theoretically[18-23] for lead halide perovskites has been named as a possible ingredient to the success of metal-halide perovskites.[24] In addition, the band structure may involve direct and indirect transitions in a very near energy range which has also been stated to be beneficial for photovoltaic efficiency[25][26]. Given that the effective mass or effective density of states are features of the band structure that are always calculated in the context of computational material screening efforts, it is of huge relevance for the community investigating novel materials for photovoltaics, whether these basic features of semiconductor band structures would be beneficial for photovoltaics at least on the level of theory where parabolic approximations to the energy vs. momentum relations of the bands are sensible. A detailed look at the key properties of solar cell absorber material, i.e. absorption, charge transport and recombination reveals that the effective mass or effective density of states enters a large number of equations that potentially affect device performance. According to Eq (12) it is clear that the effective density of state depends on effective mass, which is determined by the material, and the value of N_c can affect the density of electrons and holes directly.

$$N_c = 2 \frac{(2\pi m k_B T)^{3/2}}{h_0^3} \quad (12)$$

where, N_c is effective density of state, m is effective mass, k is the Boltzmann constant, T is temperature, h_0^3 is the Planck constant.

Through this research, we note that an increase in the density of states leads to a decrease in the efficiency and the output current, as shown in the following figures.

Table 4. shows the drawing data for effect of effective density of states for (Cb)

CB (1/cm ³)	JSC (mA/Cm ²)	Efficiency (%)
2.200E12	12.148226	9.70
2.200E13	12.146584	9.70
2.200E14	12.128397	9.68
2.200E15	12.012597	9.59
2.200E16	11.832334	9.46
2.200E17	11.784041	9.42
2.200E18	11.778389	9.42
2.200E19	11.777814	9.42

D. Effect of Different Back Contacts

Simulations have been carried out with the aid of silver (Ag), iron, copper (Cu) graphite alloy, gold (Au), nickel (Ni), and platinum (Pt). Figure 8 illustrates the impact of different back contact with efficiency. The simulated output of solar cells improves but saturates after a certain value with the rising function of the work. The majority carrier barrier height (relative to E_f) decreases due to band bending at the metal-semiconductor interface, thus making contact more ohmic [27]. As the metal's work function increases, perovskite solar cell efficiency is also increasing. Holes traveling towards the electrode are energetically unfavorable because the electric field around HTM / back contact becomes negative. For this reason, it can be expected that the lower function of the work is responsible for the Stability of efficiency. The simulation results show that Pt is one of the potential rear contact materials that can develop PSC performance

Table 7. Displays the impact on different of different metal back contact

Back contact metal	Work Function (ev)	Jsc (mA/cm ²)	Efficiency (%)
tungsten	4.5	12.187058	9.48
Ag	4.7	12.188865	9.72
Fe	4.8	12.190657	9.73
Cu	5	12.192146	9.74
Au	5.1	12.192184	9.74
Ni	5.2	12.192148	9.74
Pt	5.65	12.192148	9.74

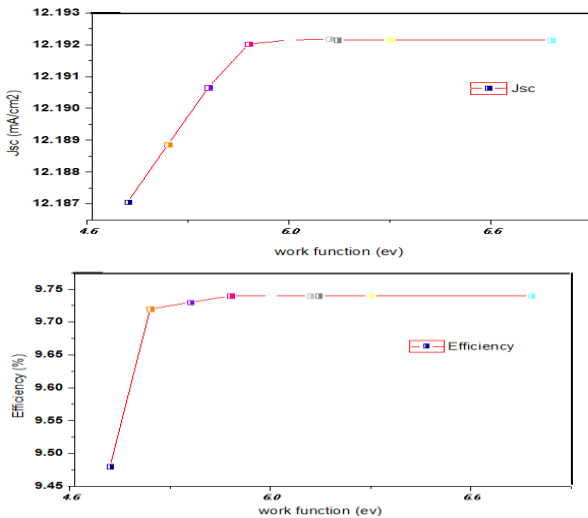


Figure 8. Increasing (Jsc,PCE) by increasing the work function for different materials

VIII. CONCLUSIONS

In this study, the thickness of the PCBM (from 100 to 2600 nm), the CB and VB of the perovskite (from 2.2E12 to 2.2E20), and the temperature were changed, and we obtained the best efficiency of 9.54% and JSC=12.011455 mA/cm² at thickness (1200 nm for PCBM, 50 nm for P3hT, 100 nm for MAPbI₃), and we found

that the optimum value of efficiency corresponding to value of VB and CB (CB=2.20E13, VB=2.200E12 for CH₃NH₃PbI₃) at temperature 263.15 K.

ACKNOWLEDGMENTS

We would like to thank Mark Burger, the electronic and information system (Elis), the University of Gent, Belgium, for providing us the free access to SCAPS simulation software, and supervisor Samir M. AbdulMohsin Thi Qar University.

REFERENCE

- [1]. C. Wehrenfennig, M. Z. Liu, H. J. Snaith, M. B. Johnston and L. M. Herz; 2014; Energy Environ. Sci., 7, 2269–2275.
- [2]. S. Zheng, G. Wang, T. Liu, L. Lou, S. Xiao, S. Yang; 2019; Materials and structures for the electron transport layer of efficient and stable perovskite solar cells. Sci. China Chem. 62 (2019) 800–809. <https://doi.org/10.1007/s11426-> [Online]
- [3]. Zhanna Zapukhlyak et al., "SCAPS modelling of ZnO/CdS/CdTe/CuO photovoltaic heterosystem", December 2020, 21(4):660-668.
- [4]. Wu, Chien-Hung Chiang & Chun-Guey; 2016; Bulk heterojunction perovskite-PCBM solar cells with high fill factor. Nature reviews. 10, pages 196–200 (2016).
- [5]. Snaith, H. J.; 2013; Perovskites: the emergence of a new era for low-cost, high-efficiency solar cells. J. Phys. Chem. Lett. 4, 3623–3630.
- [6]. Zhicai He, Chengmei Zhong, Shijian Su, Miao Xu, Hongbin Wu, and Yong Cao.; 2012; Enhanced power-conversion efficiency in polymer solar cells using an inverted device structure. Nat. Photonics, 6(9):593–597,
- [7]. Potscavage Jr, W. J. 2010; Physics and engineering of organic solar cells.
- [8]. Marchioro, A. et al. 2014; Unravelling the mechanism of photoinduced charge transfer processes in lead iodide perovskite solar cells. Nature Photon. 8, 250–255.
- [9]. Green, M. A., Ho-Baillie, A., & Snaith, H. J. 2014; The emergence of perovskite solar cells. Nature Photonics, 8(7), nphoton-2014.
- [10]. Edri et al. 2014 "Elucidating the charge carrier separation and working mechanism of CH₃NH₃PbI(3-x)Cl(x) perovskite solar cells.", Nat. Commun., vol. 5, p. 3461, Jan.
- [11]. Tanaka et al. 2003; "Comparative study on the excitons in lead-halide-based perovskite-type crystals CH₃NH₃PbBr₃ CH₃NH₃PbI₃", Sci. direct, vol. 127, pp. 619–623,
- [12]. al, Minemoto et. 2014; "Device modeling of perovskite solar cells based on structural similarity with thin film inorganic semiconductor solar cells", s.l. : J. Appl. Phys., vol. 116, no. 5, p. 054505, Aug. 2014.
- [13]. Niemegeers A, Burgelman M, Decock K. 2014; SCAPS Manual. University of Gent..
- [14]. Minemoto T, Murata M. 2014; Device modeling of perovskite solar cells based on structure - al

similarity with thin film inorganic semiconductor solar cells. *Journal of Applied Physics*. . 2014;116: 5, 054505.

[15] Noel et al. "Lead-Free Organic-Inorganic Tin Halide Perovskites for Photovoltaic Applications,". *Energy Environ. Sci.*, vol. 7, pp. 3061–3068, 2014.

[16] Liu et al. "Numerical simulation: Toward the design of high-efficiency planar perovskite solar cells," . *Appl. Phys. Lett.*, vol. 253508, no. 104, 2014.

[17] Minemoto et al. "Device modeling of perovskite solar cells based on structural similarity with thin film inorganic semiconductor solar cells,". *J. Appl. Phys.*, vol. 116, no. 5, p.054505, Aug. 2014.

[18]. Nabonswende Aida Nadege Ouedraogo, Hui Yan , Chang Bao Han ,Yongzhe Zhang., "Influence of Fluorinated Components on Perovskite Solar Cells Performance and Stability". Wiley Online Library. 01 February 2021.

[19]. Thomas Kirchartz ORCID logo*ab and Uwe Rau a. 2018; Linking structural properties with functionality in solar cell materials – the effective mass and effective density of states†. *Royal society of chemistry*, p. 23.

[20]. Snaith, F. Giustino and H. J. 2016; Toward Lead-Free Perovskite Solar Cells. *ACS Energy Lett.* 14, 2016, 2016, 1, 6, 1233–1240.

[21]. A. Miyata, A. Mitioglu, P. Plochocka, O. Portugall, J. T.-W. Wang, S. D. Stranks, H. J. Snaith and R. J. Nicholas; *Nat. Phys.*, 2015, 11, 582.

[22]. F. Staub, H. Hempel, J. C. Hebig, J. Mock, U. W. Paetzold, U. Rau, T. Unold and T. Kirchartz; 2016; *Phys. Rev. Appl.*, 2016, 6, 044017.

[23]. N. Ashari-Astani, S. Meloni, A. H. Salavati, G. Palermo, M. Grätzel and U. Rothlisberger;2017; *J. Phys. Chem. C*.2017, 121, 23886.

[24]. Y. Zhou and G. Long; 2017;*J. Phys. Chem. C*. 2017, 121, 1455.

[25]. E. M. Hutter, M. C. Gelvez-Rueda, A. Osherov, V. Bulovic, F. C. Grozema, S. D. Stranks and T. J. Savenije, *Nat. Mater.* 2017, 16, 115.

[26]. Rau, T. Kirchartz and U;2017; *J. Phys. Chem. Lett.* 2017, 8, 1265.

[27]. M. Nawaz, E.S. Marstein, A. Holt.; 2010; Design analysis ZnO/cSi heterojunction solar cell, in: *Proceedings of the IEEE Photovoltaic Specialist Conference (PVSC) Honolulu*. . . 20–25 June, 2010, pp. 2213–2218.